General Disclaimer

One or more of the Following Statements may affect this Document

- This document has been reproduced from the best copy furnished by the organizational source. It is being released in the interest of making available as much information as possible.

- This document may contain data, which exceeds the sheet parameters. It was furnished in this condition by the organizational source and is the best copy available.

- This document may contain tone-on-tone or color graphs, charts and/or pictures, which have been reproduced in black and white.

- This document is paginated as submitted by the original source.

- Portions of this document are not fully legible due to the historical nature of some of the material. However, it is the best reproduction available from the original submission.

LOW COST SILICON SOLAR ARRAY PROJECT
Large Area Silicon Sheet Task

ERDA/JPL 954654 - 77/3
Distribution Category UC-63

SGT

SILICON WEB PROCESS DEVELOPMENT

THIRD QUARTERLY REPORT

October 1, 1977 - December 31, 1977

C. S. Duncan, R. G. Seidensticker,
J. P. McHugh, P. D. Blais, and J. R. Davis, Jr.
Westinghouse Research & Development Center
Pittsburgh, Pennsylvania 15235

Contract No. NAS 954654

This work was performed for the Jet Propulsion Laboratory, California Institute of Technology, under NASA Contract NAS7-1000 for the U. S. Energy Research and Development Administration, Division of Solar Energy.

The JPL Low-Cost Silicon Solar Array Project is funded by ERDA and forms part of the ERDA Photovoltaic Conversion Program to initiate a major effort toward the development of low-cost solar arrays.

Westinghouse R&D Center
1310 Beulah Road
Pittsburgh, Pennsylvania 15235

LOW COST SILICON SOLAR ARRAY PROJECT
Large Area Silicon Sheet Task

ERDA/JPL 954654 - 77/3
Distribution Category UC-63

SILICON WEB PROCESS DEVELOPMENT

THIRD QUARTERLY REPORT

October 1, 1977 - December 31, 1977

C. S. Duncan, R. G. Seidensticker,
J. P. McHugh, P. D. Blais, and J. R. Davis, Jr.
Westinghouse Research & Development Center
Pittsburgh, Pennsylvania 15235

Contract No. NAS 954654

This work was performed for the Jet Propulsion Laboratory, California Institute of Technology, under NASA Contract NAS7-1000 for the U. S. Energy Research and Development Administration, Division of Solar Energy.

The JPL Low-Cost Silicon Solar Array Project is funded by ERDA and forms part of the ERDA Photovoltaic Conversion Program to initiate a major effort toward the development of low-cost solar arrays.

Westinghouse R&D Center
1310 Beulah Road
Pittsburgh, Pennsylvania 15235

TECHNICAL CONTENT STATEMENT

This report contains information prepared by WESTINGHOUSE ELECTRIC CORPORATION under JPL subcontract. Its content is not necessarily endorsed by the Jet Propulsion Laboratory, California Institute of Technology, National Aeronautics and Space Administration or the U. S. Energy Research and Development Administration, Division of Solar Energy.

ABSTRACT

During the report period, the experimental phase of the program was oriented toward developing growth configurations which produced crystals having low residual stress levels. It was found that some slot designs, especially thick lids with narrow slots tended to produce crystals with high residual stress, however these lids also were conducive to melts with minimal temperature fluctuations and relatively flat temperature profiles. Conversely, it was found that lid designs which could be characterized as having wide slots and thin section would grow crystals with low residual stress, but the temperature fluctuations in the melt were greater and the crystals tended to spontaneously pull free of the liquid. Work is presently underway to develop designs which combine the advantages of each design.

Several runs were also made to evaluate the properties of a 106 mm diameter round crucible which in principle should have a superior thermal profile. In practice, it was found that this design had greatly enhanced temperature fluctuations arising from convection in the melt. After seven runs with this system, further work was postponed. in order to accelerate investigations of the susceptor lid designs.

Thermal modeling efforts were directed to developing finite element models of both the 106 mm round crucible and an elongated susceptor/crucible configuration for the new furnace system. The model for the larger round crucible was completed and predicted a very satisfactory temperature distribution. The model for the elongated system is nearing completion. Additionally, the separate thermal model for the heat loss modes from the dendritic web itself was examined for guidance in reducing the thermal stress in the web. It gave direction in reducing the thickness of the lid and increasing the width of the slot. While this strategy proved successful in achieving the desired

reduction of residual stress, other melt problems such as "pull-out" were accentuated. Nevertheless, the critical parameters have been identified and concepts are now being developed for hybrid designs which will reduce the thermally generated stress while maintaining good melt thermal conditions.

An economic analysis has been prepared in order to evaluate the silicon web process present and expected future status as related to the JPL LSSA 1982 and 1986 price goals. This analysis considers but is not limited to the wafer value-added cost. It further includes evaluation of the polysilicon cost requirements of the process since those requirements vary greatly among the competing processes. The analysis concludes that the present rate of growth capability can satisfy the 1982 goal with considerable margin to spare. It is also shown that the process will need a rate of growth increase of as small as a factor of two in order to satisfy the 1986 combined polysilicon and wafer price goal.

TABLE OF CONTENTS

LIST OF ILLUSTRATIONS

LIST OF TABLES

LIST OF CURVES

1. INTRODUCTION

The overall intent of this program is to further develop the dendritic web crystal growth process to the extent that it supports the economic goals of the Large Area Silicon Sheet Task of the Low-Cost Silicon Solar Array Project.

The ability of this process to produce crystals for high efficiency solar cells, 14 percent AM-1 or higher, is well known and has been demonstrated in pilot production and in this program. The prior state of development of the process did not, however, have sufficient throughput to satisfy the cost goals of the LSSA Project.

Consequently, a key goal of this program is to increase the throughput of the process in terms of greater width (to as great as 7.5 cm), greater speed (to as great as 7.5 cm/min) and greater length (to > 10 meters) within the web thickness range of 100 to 200 μm. These goals are being sought via two growth facilities: an existing facility which is undergoing continued development and a new facility now in the construction and assembly phase.

The existing facility has produced crystals to 2.8 cm width and 3 meters length. Growth rates for useful material in the range of 100 to 200 μm thickness have reached 3.0 cm/min although some experimental growth at rates as high as 10 cm/min have been achieved for very thin web. The goal of this phase of the program is to achieve a growth width equal to the 5 cm dimensional capacity of the facility and a growth rate of 5 cm/minute. Both facilities have provision for adding polycrystalline silicon feed material to the melt for achieving a quasi-continuous growth.

The new facility, now nearly complete, has capacity to meet the full throughput goals stated above. The growth run experiments with both facilities will be used to identify the necessary on-line process

parameter measurements and control.

Computer thermal models are a critical factor in the successful development of the process. The models are verified and refined initially by temperature measurements of sensors located in the thermal system and subsequently by correlation with actual web growth results. As the program progresses, a large volume of data is being generated and related to growth conditions, crucible system geometry, crystal quality, etc.

During the process development period with both facilities the web crystals grown will be used for several purposes. The growth is routinely selected and evaluated in terms of its dimensional, crystalline, electronic, and solar cell properties. For solar cell evaluation a "standard" fabrication procedure suitable for web crystals is used. Crystals are also provided for another program goal which is developing improved solar cell fabrication techniques especially suited to web crystals. Finally, selected web crystals and solar cells are sent to JPL.

Growth runs will also be performed to determine the interaction of controlled amounts of selected impurities with growth conditions and parameters. This evaluation will be performed in a third web growth facility which is also used for other web programs.

An economic analysis has been prepared to evaluate the present and future status of the silicon dendritic web growth process with reference to the JPL 1982 and 1986 price goals.

2. TECHNICAL DISCUSSION

2.1 Experimental Web Crystal Growth

The major objective of the experimental crystal growth activity during this report period has been to develop growth conditions conducive to pulling wider dendritic web crystals. Specifically, the emphasis was on obtaining conditions under which the web crystals would grow long enough to widen to the steady state width capability of the system. Data discussed in the previous quarterly report(1) indicated that the temperature profiles in the melt were adequately flat for the growth of dendritic web crystals of the order of 35 mm wide or more. In practice, however, the maximum widths achieved were between 25 and 27 mm because the crystals deformed and the pull had to be terminated even though the crystals were still widening at a constant rate. This deformation of the ribbon and the concommitant loss of crystal quality appeared to be the most serious obstacle to achieving increased area throughput in the dendritic web process and the efforts to eliminate the problem were the chief tasks during the period.

At the beginning of the report period, it had been established that most of the dendritic web crystals which had been grown up to that time had moderate residual stresses of about 2×10^8 dynes/cm^2 (2900 psi). This included not only crystals grown on the current program but also crystals grown in previous studies. It was suspected that the mechanisms which gave rise to the residual stress in the web might also be the mechanisms which caused the gross warping of the ribbon. Further, it was hypothesized that the cause of the residual stress was the non-linearity of the temperature profile in the growing web crystal in analogy with the effects found by workers with other ribbon growth techniques. The research effort was thus focused on the evaluation of

thermal designs that had the potential for reducing thermally induced stress in the growing crystals.

The thermal model for the heat loss from the growing web not only allowed the thickness-velocity-undercool behaviour of the web to be calculated, but also could be interrogated to give the temperature distribution and the z-derivatives of the temperature in the web. According to the model, the second derivitive of the temperature is a rapidly varying quantity in the first centimeter or so of the ribbon, and in fact changes sign (see the later discussion of the thermal modeling). In general, however, the magnitudes of the curvature variations could be reduced by changing the design parameters such as the thickness of the lid, the width of the slot, and the distance of the melt below the lid. Thinner lids, wider slots, and closer melts all tend to reduce the magnitude of the second derivative. If indeed the curvature of the temperature profile in the crystal is responsible for the residual stress, then making changes in the lid ought to change the residual stress.

During the reporting period, a number of lid designs were evaluated: 13 different slot/lid configurations were tried over the course of 30 furnace runs and a total of 80 crystals were grown. Appendix 1 summarizes the growth data for these crystals. Appendix 2 contains an ad hoc summary of the lid design classifications; a specific slot designation consists of an initial number which specifies the opening and one or more letters which identify the vertical cross section, e.g. slot 3A. This scheme of identification is not intended to supplant the formal engineering drawings for the susceptor lids, but rather to serve as an aid for day to day engineering and analytical use.

The results of the growth experiments are subject to somewhat ambiguous interpretation. Crystals grown from lids which were expected to produce lower thermal stresses indeed had significantly lower residual stresses; in some cases the stress was almost two orders of magnitude lower than previously measured. However, achieving lower residual stresses did not necessarily produce longer crystals or eliminate

deformation. Instead of having most crystal pulls terminated by the deformation of the ribbons, spontaneous pull out became a second terminating cause. Apparently the same conditions that led to lower residual stress adversely affected the thermal geometry in the melt and enhanced the convectively generated thermal fluctuations. For this reason the most recent work on this aspect of web growth is directed toward developing lid designs which will permit the growth of wide, low stress crystals and still minimize pull out.

In addition to the experiments on lid design using the 79 mm diameter crucible, seven runs were made with a 106 mm diameter crucible; the suceptor height and diameter was the same in both cases. Due to an unrecognized drafting error, the crucibles used for the first three 106 mm runs were too shallow and could not be loaded properly. As a result, the liquid silicon did not wet the crucible uniformly and the resulting lop-sided melt was very unstable. New deeper, crucibles were obtained and the wetting problem was eliminated. Nevertheless, the melt proved to be thermally very unstable, although the mechanical stability was improved. It was not possible to grow web crystals more than a few tens of centimeters in length before they pulled out spontaneously. Thermocouple probing of the melt revealed large intrinsic temperature fluctuations in the liquid ($\pm$ 1.5°C) which was consistant with the lack of ability to grow much material. After four runs with the new, deeper 106 mm crucibles, it became apparent that there were problems associated with this crucible design which would require considerable efforts to fully characterize. Because it was felt that such effort could be much more productive if applied to more intensive work on lid design on the letter characterized 79 mm diameter system, further efforts on the 106 mm system were discontinued.

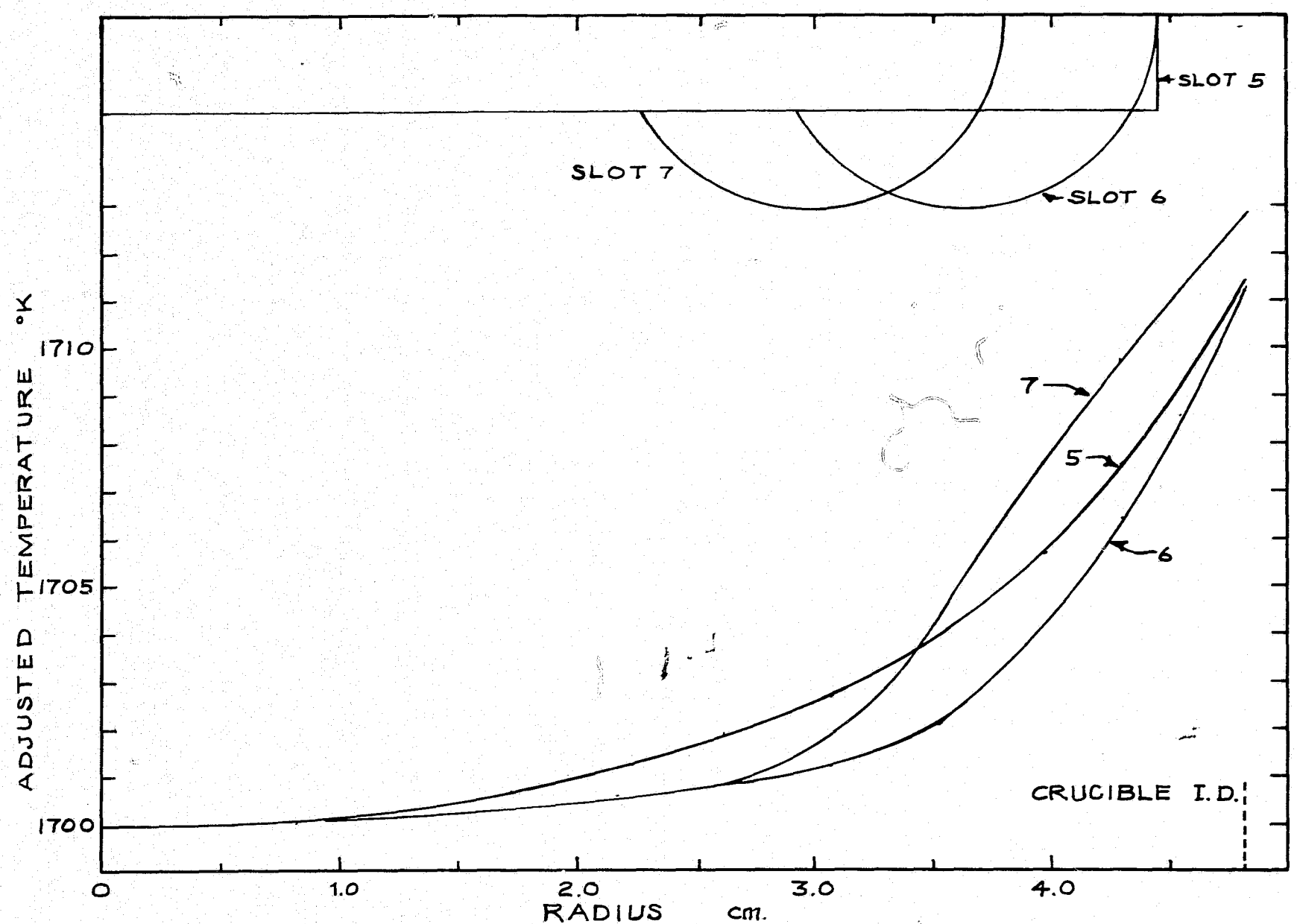

Fig. 1 Temperature profiles in a 106 mm crucible.

PROTOTYPE SUSCEPTOR, Mk. III

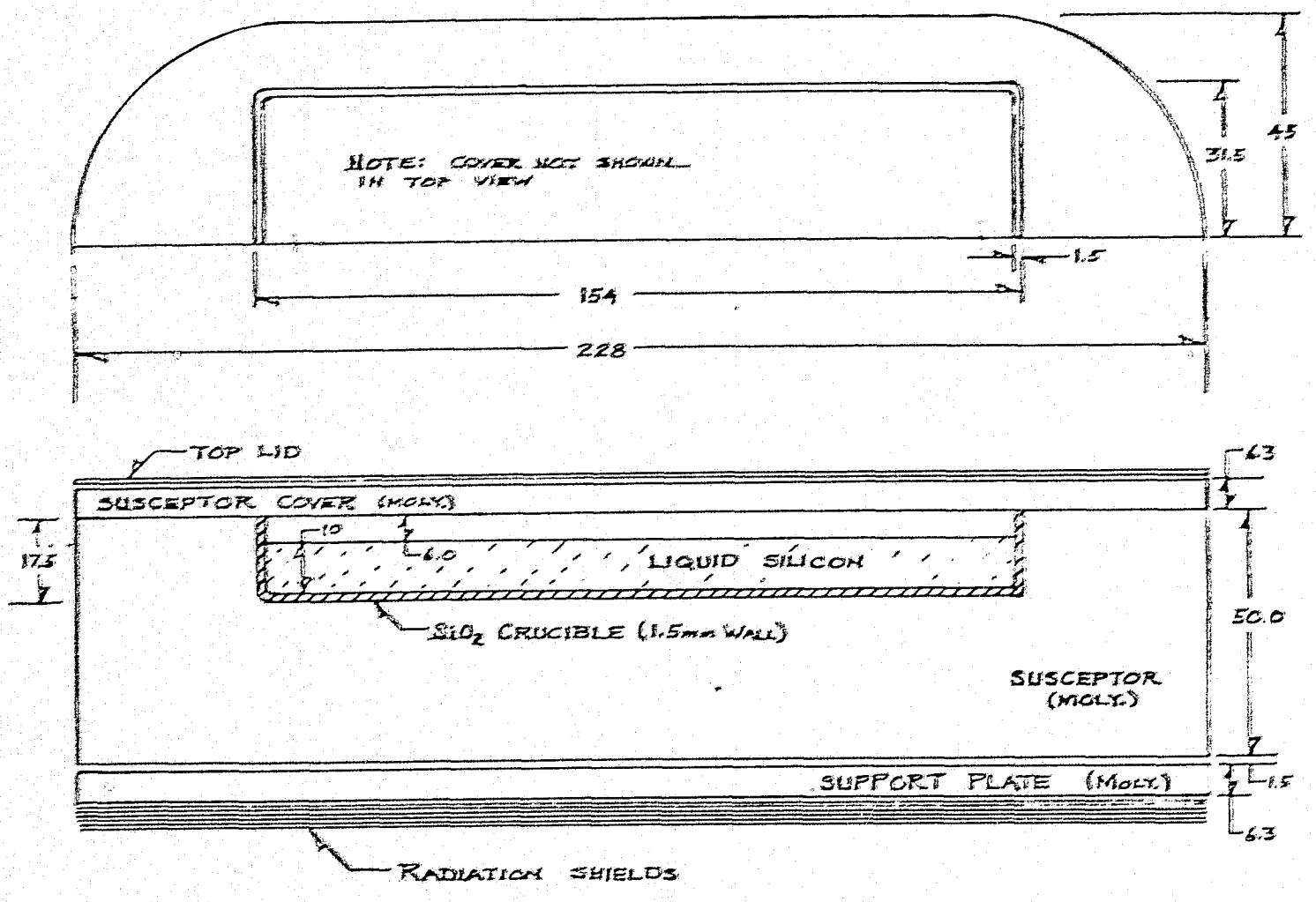

Figure 2

2.2 Thermal Modeling

During the reporting period, two finite element models were undertaken to develop melt temperature profiles. The first was a model of a susceptor and crucible system similar to the 79 mm diameter crucible system previously modeled except that the crucible had a diameter of 106 mm. The second thermal model under development is an enlongated crucible and susceptor for use in the new furnace facility.

The model for the 106 mm round crucible was relatively easily constructed. The computer code used for the finite element analysis actually creates the elements, and the configuration used for the 76 mm diameter crucible was simply modified by specifying coordinate transformations and eliminating some of the element series. Several slot configurations for the lid were modeled and the results are shown in Fig. 1. Two of the designs appeared to give acceptably flat temperature profiles, and Design No. 6 was fabricated for use with system. Unfortunately, the convectively generated temperature fluctuations in the melt precluded experimental verification of the results, however the limited growth results did not contradict the conclusion that a flat gradient existed in the melt. The thermal model did indicate that the temperature difference between the melt center and the crucible wall was somewhat greater than in the 79 mm crucible and this larger temperature difference as well as the larger liquid dimensions of the system might well have contributed to the enhanced convection.

A simplified representation of the elongated system is shown in Fig. 2. Developing the finite element model for this configuration is a more complicated task than developing the model for the round susceptors, since the axial symmetry cannot be used in generating the element code. The development of this model is still in process.

Another aspect of the thermal modeling effort has been the application of the thermal model for the heat loss from the web to the problem of the thermally generated stress in the ribbon crystals. Not

only does the model permit the evaluation of the velocity-thickness-undercooling behaviour of the system, but it also generates the temperature distribution and several derivatives of the temperature distribution in the growing web.

When the model was examined, it was found that the second derivative went through a minimum and maximum as shown schematically in Fig. 3. Here the value of d^2T/dz^2 is plotted against T rather than z since it has been tacitly assumed that curvature in the temperature profile at temperatures less than 1300°K will introduce elastic rather than plastic strain and thus will not contribute to residual stresses in the crystal. The physical reasons for the alternating behavior of the second derivative can be seen from Fig. 4. Near the growth front, the ribbon is hot enough that it has a net heat loss to its surroundings (the hot cavity, the hot lid, and the cool ambient). While still in the cavity, the ribbon cools sufficiently that the crystal actually receives a net heat input from the surroundings. Finally, when the web nears the top of the slot, the cool ambient becomes predominant and for the balance of the length, there is a net heat loss.

The general shape of the second derivative distribution is unchanged by changes of the slot geometry, however the magnitude and to some extent the distribution of the maxima and minima are varied by changes in such parameters as the thickness of the lid, the width of the slot, and the distance of the melt below the lid. Generally, wider slots, thinner lids and closer melts all tend to decrease the magnitude of the second derivative excursions. To a large extent, changes in the lid thickness have no great effect on the temperature distribution in the liquid. Increases in slot width, however, increase the total heat loss from the liquid and increase the dip in the temperature distribution in the melt. In addition, the increased slot width increases the heat loss from the meniscus near the growth front which fosters the generation of extra dendrites or "thirds" as they are called. Similarly, having a melt too close to the lid also fosters the generation of thirds.

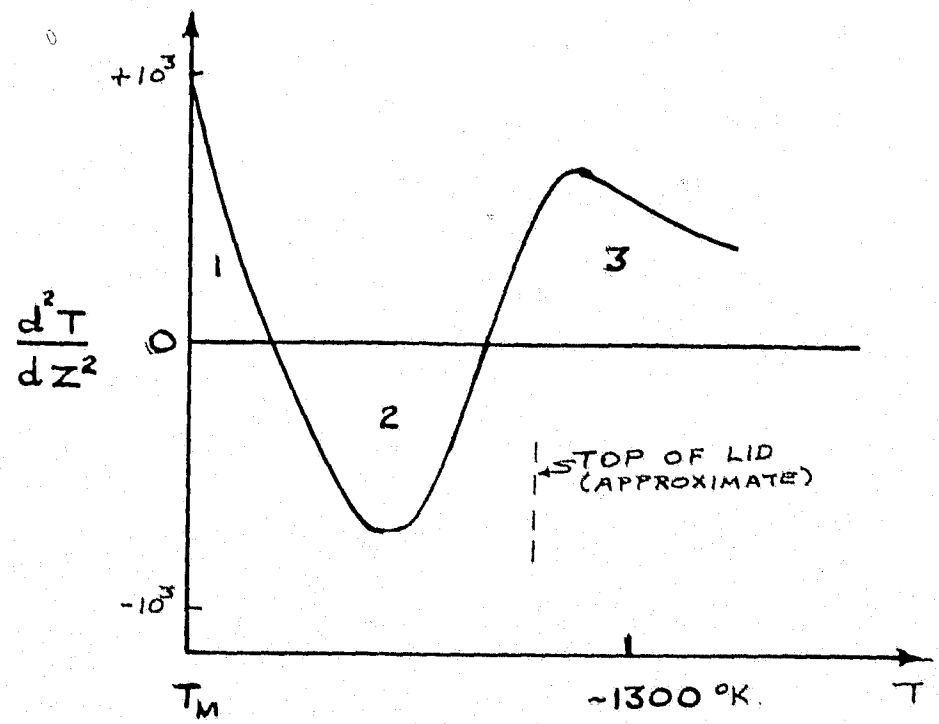

Fig. 3 Schematic Behavior of d^2T/dZ^2 in Web Crystal

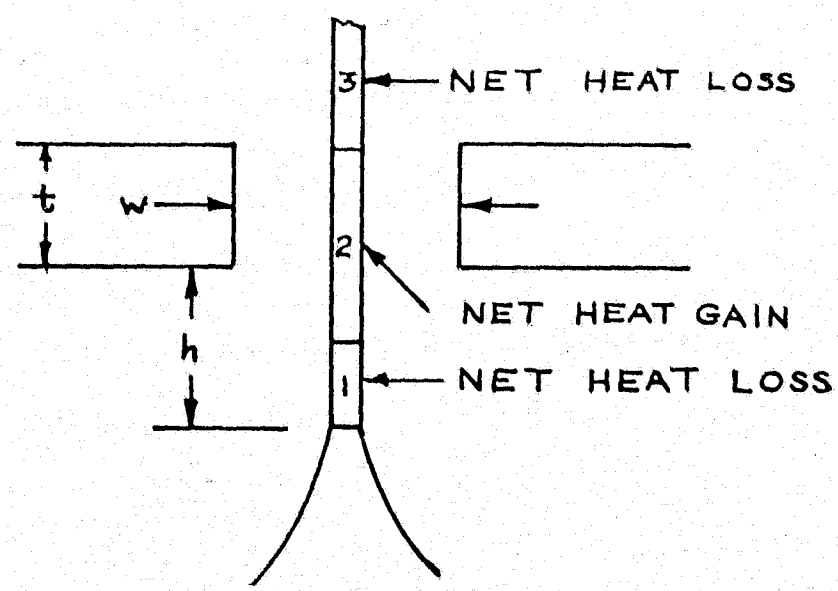

Fig. 4 Physical Basis for Curvature in Temperature Profile

The development of a satisfactory lid design therefore becomes a matter of arriving at an compromise between a design that does not produce high stresses in the growing web and which still gives acceptable temperature distributions in the meniscus and in the melt as a whole. The conceptual basis for such an optimized design is shown in Fig. 5. A thick lid with a narrow slot (typified by slot 22D) experimentally tends to give reasonably wide web having relatively high residual stresses. Thinner lids with wider slots (typified by slot 4C) could be expected to generate webs with lower residual stress, but in practice it was found that the melt thermal convection increased and the crystals tended to pull out spontaneously. Our initial approach at a combined design was thus to use a physically thick lid with a beveled slot -- a "pseduo thin lid" with a "pseudo wide slot".

The physically thick lid is hotter and has a more uniform temperature distribution than the thinner lids. This feature, combined with the smaller area of the slot should generate a shallower and flatter temperature distribution in the melt. The region of the crystal near the growth front, however, has a larger view of the ambient than it would in an unbeveled slot.

Some confirmation of this behavior is given by the data presented in Fig. 6. The measured residual stress is plotted as a function of the square of crystal width for several lid designs. Several general features are apparent. First, there is a moderate amount of scatter in the data. Part of this scatter could arise from uncertainties in the measurements of the split width. This is especially true with those crystals having very small residual stresses. Another source of variability could come from the variation of melt height from crystal to crystal, a factor which would be especially bothersome in the data related to the thin lids. Depending on the dimensions of the crystal, something between 8 and 15 grams of silicon are removed from the melt during a pull, and the melt level drops about 1 mm for each 11 grams of liquid. If the lid is "thick", then the melt level effect is small, however if the lid is "thin", then changes in melt level have a stronger effect.

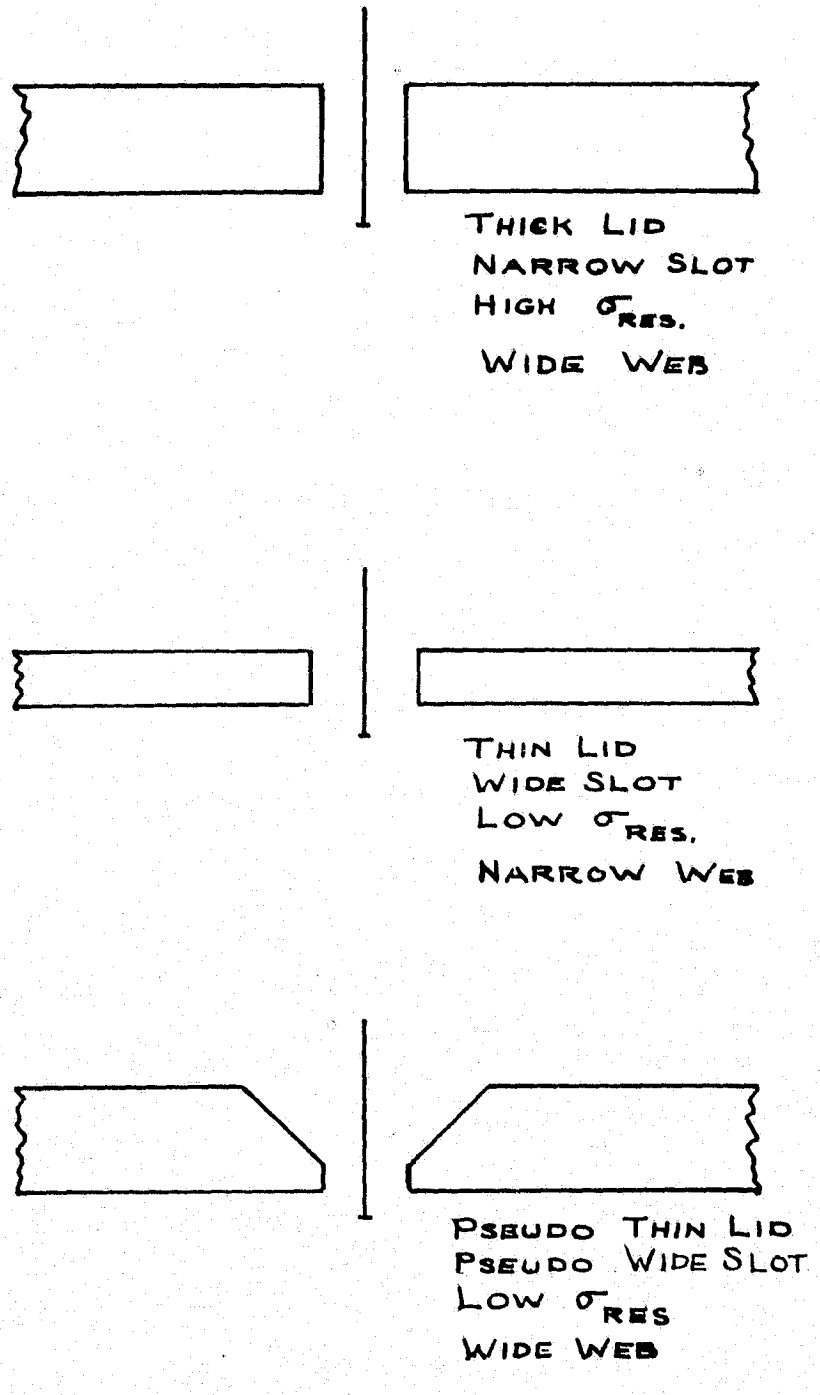

Fig. 5 Conceptual Development of Optimized Slot Cross Sections.

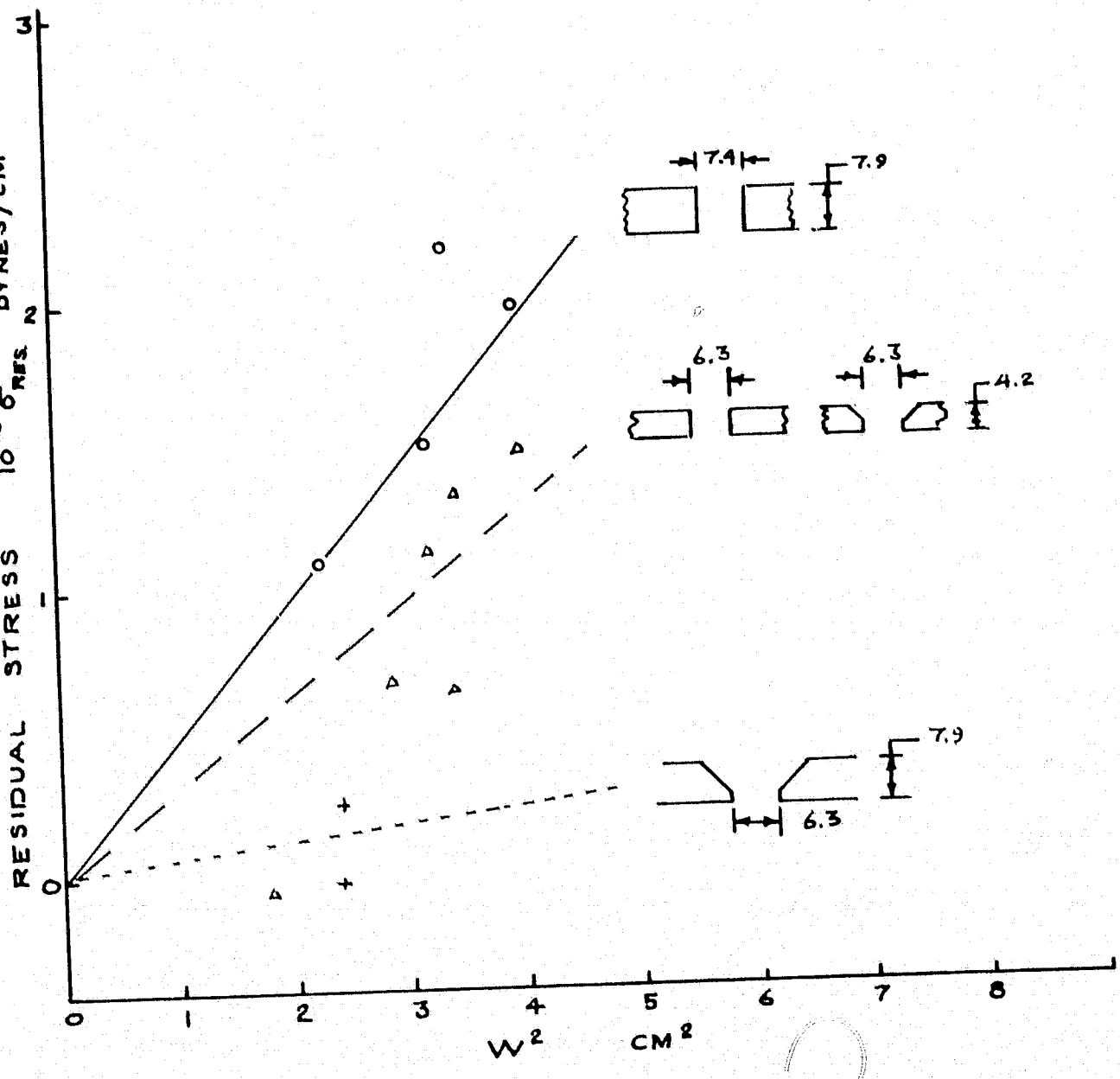

Fig. 6 Residual Stress Data for Various Slot Profiles

Another feature to be noted from the data is the moderately good dependence of residual stress on the square of the ribbon width. Since this is the sort of variation which might be generated by curvature in the vertical temperature profile, it is suggestive that indeed this mechanism is acting. Further, it permits σ_{res}/w^2 to be used as a "figure of merit" in evaluating lid configurations. Some data for crystals grown from "thick" and "thin" lids is shown in Table 1.

Finally, the data shows that there is a strong relation between the cross section of the lid and residual stress. Since the thermal model indicates that the region of large curvature in the temperature profile lies in the portion of the crystal below the top level of the lid, it is perhaps not surprising that the lid should have a strong effect. The most important aspect would seem to be that it is possible to reduce the thermal stress as much as has been done. This gives some reassurance that lid designs with suitable combinations of properties can be engineered.

2.3 Material Characterization

The data on the residual stress characteristics of a number of web crystals has been given in the section on thermal modeling. In analyzing that data it was found that the vertical profile of the slot in the susceptor cover was a very important parameter. In the case of the web widening rates, which are listed in Table 2, the profile of the slot seems to make little difference. With the exception of R181 and crystal R193-1, all of the rates are nearly the same: dW/dt:12 - 16 x 10^{-3} cm/min. Run R181 was made with the 106 mm crucible and the lid had a wide (8 mm) slot with large (15.9 mm) "dogbone" holes; this configuration had dW/dt 24 x 10^{-3} cm/min. This rate would be consistant with the flat temperature profile expected in the melt, however it should be noted that the large slot opening in the lid is also conductive to a rapid widening rate. As has been noted, dendritic web growth from this configuration is difficult and no additional data has been obtained. Crystal R193-1 was the first crystal grown from a high melt and the additional heat loss from the melt surface near the dendrites evidently also accelerates the

TABLE 1

Residual Stress Data for Crystals Grown from Thick and Thin Lids

Crystal	Lid/Slot Design	σ_{res}/w^2 dyne/cm	w^2 cm^2	t μm
	(thick lids)			
R172-5	22D	4.7×10^7	2.25	173
R180-4	22D	6.4	3.38	107
R186-2.4	22D	3.2	3.28	126
R188-2	22D	4.6	3.09	140
R193-4	22D	5.0	3.98	119
		av. 4.8±1.0		
	(thin lids)			
*R129-1.4(w)	1C	4.1	4.67	183
R129-1.4(wo)	1C	3.3	3.08	183
R189-1	5C	-0.23	1.88	160
R191-2	5C	0.90	4.2	116
R199-2.2	1A	-0.3	1.8	135
R199-4.6	1A	1.9	3.35	126
R201-4	3C	2.3	2.84	124
		av. 1.7±1.6		

*Measurements on R129-1.4 with (w) and without (wo) the bounding dendrities.

TABLE 2

Widening Rate of Dendritic Web Crystals

Crystal Number	Widening Rate $10^3 \times \frac{dW}{dL}$	Thickness μm	Widening Rate $10^3 \times \frac{dW}{dt}$ cm/min	Remarks/Lid Design
R176-2	5.85	155	5.3	4M
R177-3	6.9	169		4M
R178-2	8.1	147	15.7	4M + 2 shields
-3	6.94	140	12.5	
R180-1	6.9	106	15.3	22D
-2	6.95	111	13.5	
-4	6.85	107	12.3	
R181-1	11.9	144	26.4	106 mm crucible, Lid 6D
-2	9.6	225	23.9	
R184-1	8.55	145	16.6	22D
-2	8.0	150	13.0	
R185-1	6.24	147	13.0	22D
R186-1	7.7	130	16.0	22D
-2	7.5	165	14.6	
-3	7.4	112	14.4	
R188-1	8.33	203	13.8	22D
-2	5.52	140	9.16	
-3	7.38	150	11.2	
-4	3.08	145	4.7	
R189-1	5.78	165	11.2	5C + 2 shields
R190-1	8.02	170	16.7	3E (Inverted)
-2	7.85	116	16.3	
-3	6.55	147	11.8	
R193-1	9.25	233	17.9	22D, High starting melt
-2	7.50	143	16.6	
-3	5.05	125	11.2	
-4	6.05	128	13.4	
R194-1	7.05	150	14.7	22D
-2	7.80	153	15.1	
R199-2	6.1	140	13.5	1A
-4	6.0	126	13.3	
R200-3	5.4	63	17.3	1C
R201-4	6.25	114	12.1	3N
R202-1	6.4	124	16.8	2C

widening.

In addition to dimensional characterization, there has been some effort to relate the structural perfection of the web crystals to the efficiency of solar cells produced on them. Samples of the crystals were fractured and the twin structure evaluated. In several cases, x-ray topographic studies of the dislocation distribution were also done. So far, the results are ambiguous, but several trends can be seen. First the dislocation structure *per se* seems to have minimal effect; cells with efficiencies of about 12.5% can be made on material with large dislocation densities. Second, distortions in the twin structure such as changes in the twin spacing across the width of the crystal or the generation or loss of a twin lamella is a more serious defect; such material frequently is associated with cells having 10 to 11% efficiencies. These are not invariable observations and one cell having an efficiency of 14.3% was fabricated on material having five twin planes. Nevertheless, defects in twin structure require a low angle grain boundary or stacking fault, and such structures apparently degrade cell performance. These studies of the effects of twin structure are continuing especially the causes for degradations.

2.4 Economic Analysis

Introduction

An economic analysis of the silicon web growth process has been prepared in order to evaluate its present and anticipated future status with respect to the JPL LSSA project goals and, additionally, to identify the most productive direction for further development. Using the most recent technical information, the analysis was prepared according to the JPL Interim Price Estimation Guidelines (IPEG). The analysis data has been plotted in the form of curves to show present and future technology development with respect to the JPL 1982 and 1986 goals.[2]

Data and curves were prepared in three distinct parts: Polysilicon Costs, Wafer Costs, and Combined Polysilicon and Wafer Costs.

Polysilicon Cost

The silicon web growth process is uniquely economical in its use of silicon. One of its most important characteristics is inherently thin growth. Web ribbon grown during this program is typically of 5 mils (.125 mm) thickness, which is a cost advantage factor of 2 or greater as compared to competing ribbon growth methods. The cost advantage may be even larger in view of the fact that silicon web has been grown reliably at 4 mils (.100 mm) thickness and developmentally at 2 mils (0.050 mm) thickness. Also, cells have been prepared experimentally from 2 mil thick material using fabrication techniques not yet fully developed. For this analysis a thickness of 6 mils (.150 mm) was assumed.

Silicon ribbon from various growth processes, including silicon web, is of the most economical growth shape for solar cell fabrication. Ribbon inherently provides a rectangular shape for cell fabrication and results in virtually no waste of silicon from cutting to cell size and provides the highest possible cell packing density in modules and solar panels.

Unique among all wafer manufacturing methods, silicon web grows with a very flat faceted surface which requires no material removal (waste) by lapping polishing or etching. Only a mild surface cleaning is required as a preparatory step prior to cell fabrication.

High cell solar conversion efficiency is another very important economic advantage of the silicon web process. The web process can produce cells of the highest efficiency ($\sim$ 15% AM 1) which is substantially higher than cells fabricated from other ribbon growth processes and equalled only by cells produced from Czochralski grown crystals.

The polysilicon cost of the silicon web growth process as related to the JPL 1982 dollars per peak watt goal is given in Curve No. 1. The cost is shown for four and six mil thick web ribbon as a function of polysilicon price. For either thickness the dollars per peak watt cost falls well below the 1982 JPL goal even when using polysilicon at or above actual 1978 market prices. Lower polysilicon prices which may be effected by 1982 will of course further reduce the polysilicon contribution to the 1982 module cost to a value far below the 1982 module dollars per peak watt price goal.

Curve No. 2 relates the polysilicon cost of the silicon web process to the 1986 goal. As is shown for six mil thick silicon web, the 1986 JPL polysilicon dollars per peak watt cost goal will be satisfied at a polysilicon price of $25 per kilogram. Four mil thick silicon web will satisfy the cost goal at a polysilicon price of about $35 per kilogram. In the event that a lower polysilicon price is achieved by 1986 the result will be a polysilicon dollars per peak watt contribution correspondingly lower than the 1986 goal.

Wafer Cost

In addition to the technical and cost advantages discussed in the preceeding paragraphs, the silicon web process has the added advantage of inherently stable growth and of being adaptable to automated growth requiring a very small labor content. The adaptability to automated growth has been shown in experiments in which silicon web has been grown manually for periods up to two hours with no operator adjustments of any kind. Eventually the changing melt level created sufficient thermal changes to interrupt the growth. Manually adjusted growth has produced continuous uninterrupted growth length as great as 28 feet until the crucible was essentially depleted of silicon. Continuous unadjusted (automatic) growth will require continuous melt replenishment. The feasibility of continuously feeding silicon into the melt during web growth has been demonstrated but has not yet been developed into a working system. Automated growth was assumed in the calculation of this cost analysis.

Another advantage of the silicon web process is the relative simplicity and resultant low cost of the growth apparatus. Still another advantage is the comparative small size of the melt and the heated zone. Crucibles are within the $10 to $20 price range as compared to hundreds of dollars each for some competing processes. The small heated zone results in power economy because the amount of wasted heat is greatly reduced.

The wafer cost for silicon web as related to the JPL 1982 goal is shown in Curve No. 3. A one day growth cycle is seen to satisfy the 1982 goal at the present rate of technology; a longer growth cycle will result in a dollars per peak watt cost considerably below the goal.

The 1986 costs are given in Curve No. 4 which show that a factor of three improvement is required in order to meet the 1986 goal if a three day growth cycle is used. A somewhat lesser improvement would be necessary if a longer growth cycle is used.

Dollars per square meter wafer costs are given in Curve Nos. 5 and 6 which show a cost to goal relationship similar to the curves representing dollars per peak watt.

Combined Polysilicon and Wafer Costs

Wafer cost alone does not fully evaluate the economic worth of a wafer process. The polysilicon utilization efficiency of a wafer process also has a strong bearing on its economic value. For this reason the combined polysilicon and wafer costs for the silicon web process are given in Curve Nos. 7 and 8 with reference to the JPL combined goals for polysilicon and wafers. Curve No. 7 shows that the present area growth rate technology for silicon web more than satisfies the 1982 goal at a polysilicon price of $60 per kilogram. As lower polysilicon prices come into effect a corresponding improvement in dollars per peak watt cost will result.

Curve 694243-A

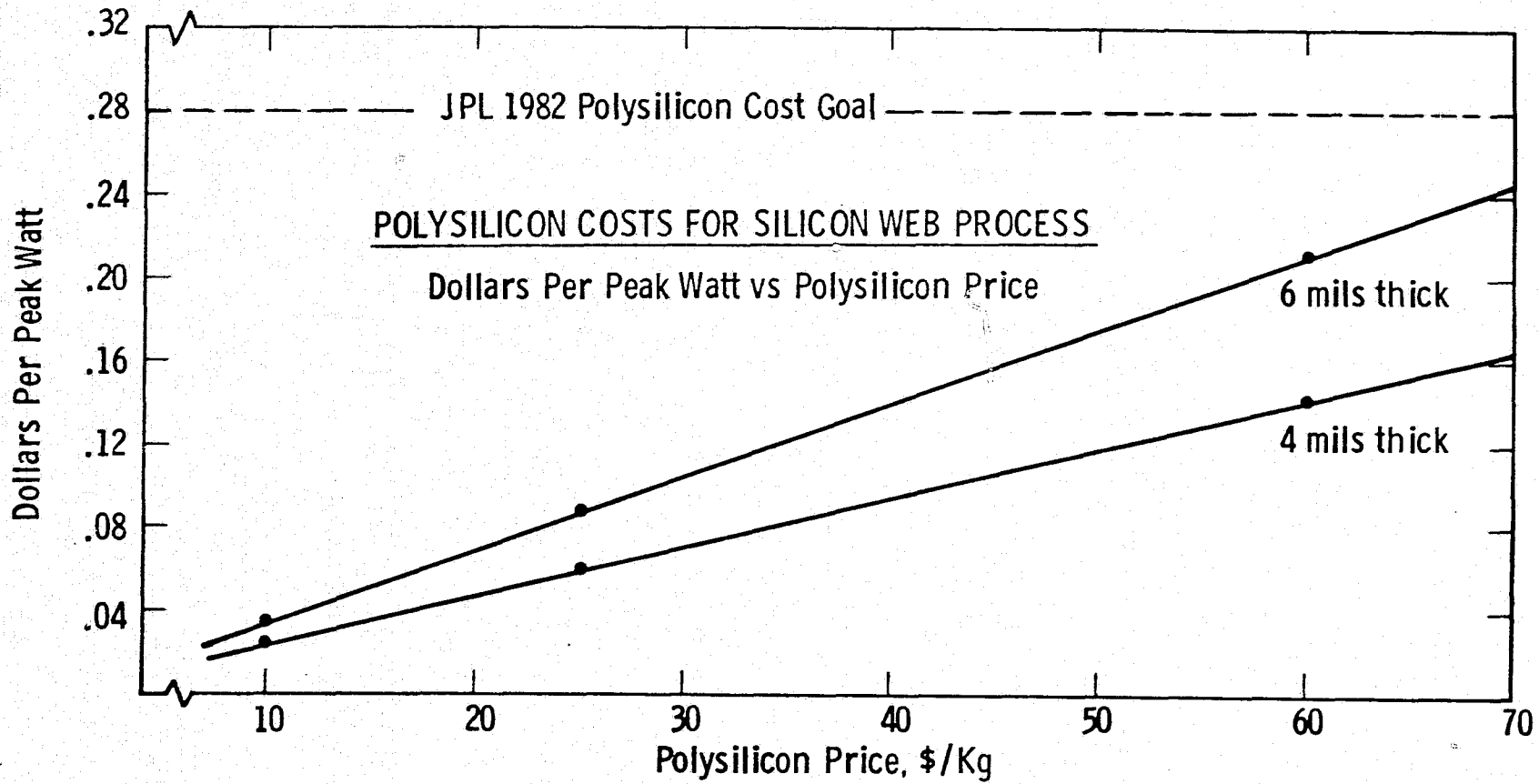

CURVE NO. 1

Curve 694242-A

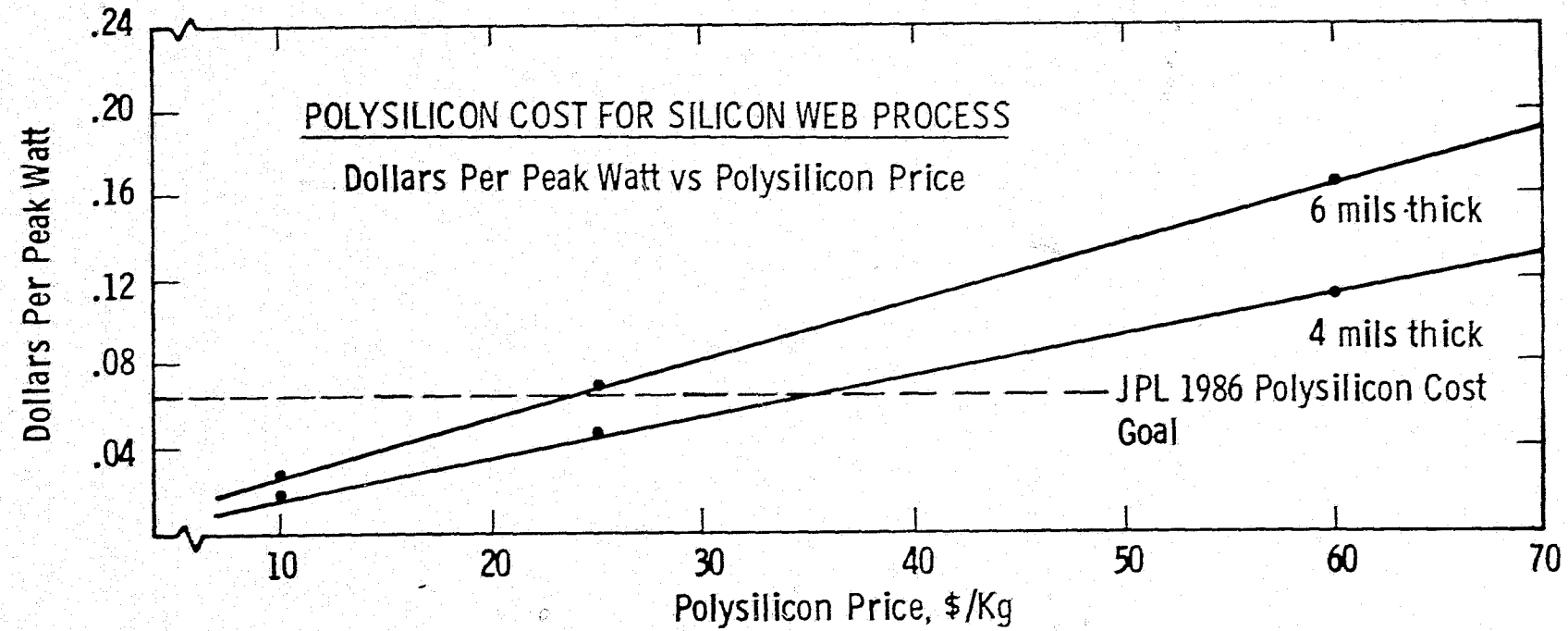

CURVE NO. 2

Curve 693533-A

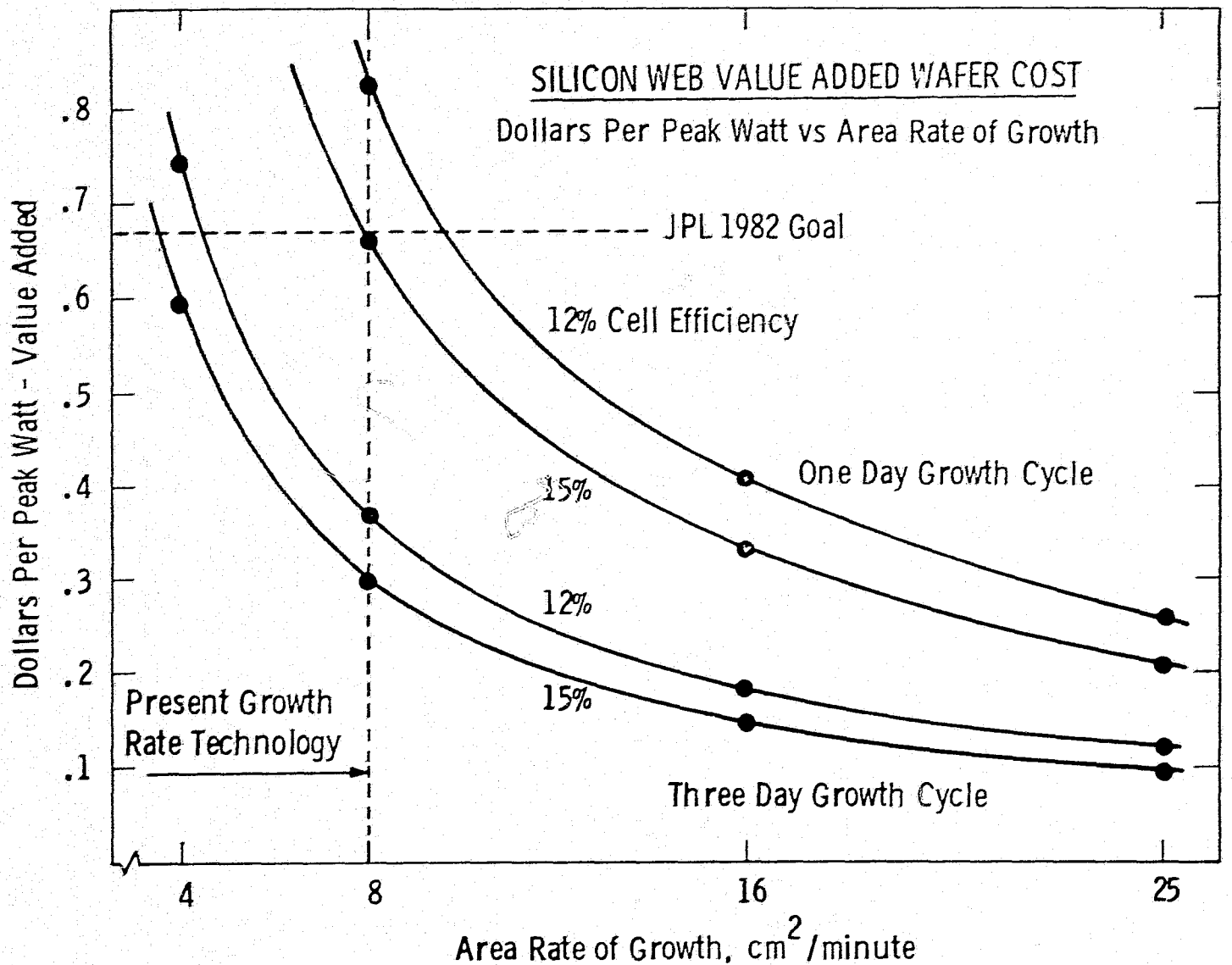

CURVE NO. 3

Curve 693534-A

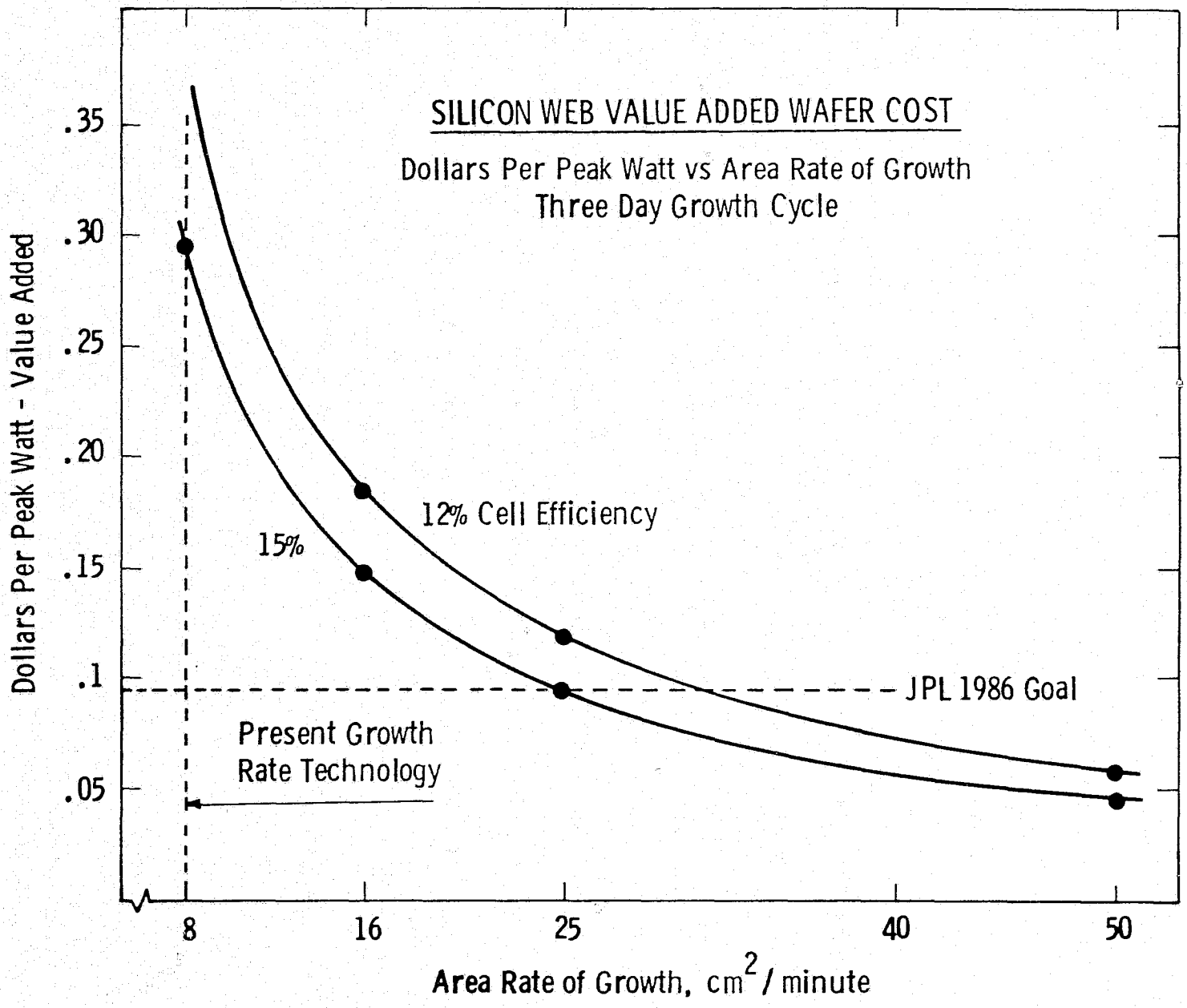

CURVE No. 4

Curve 693532-A

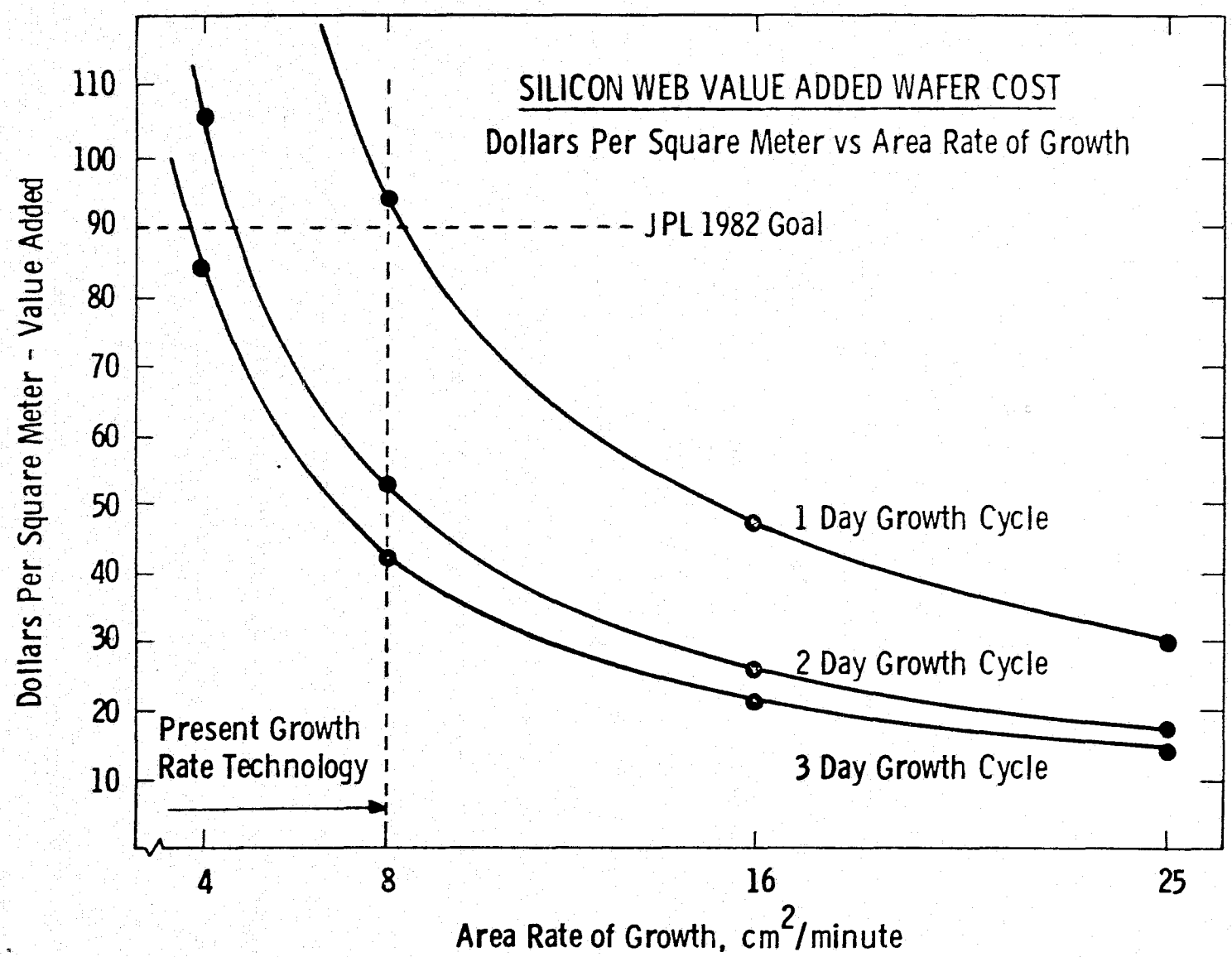

CURVE No. 5

Curve 693531-A

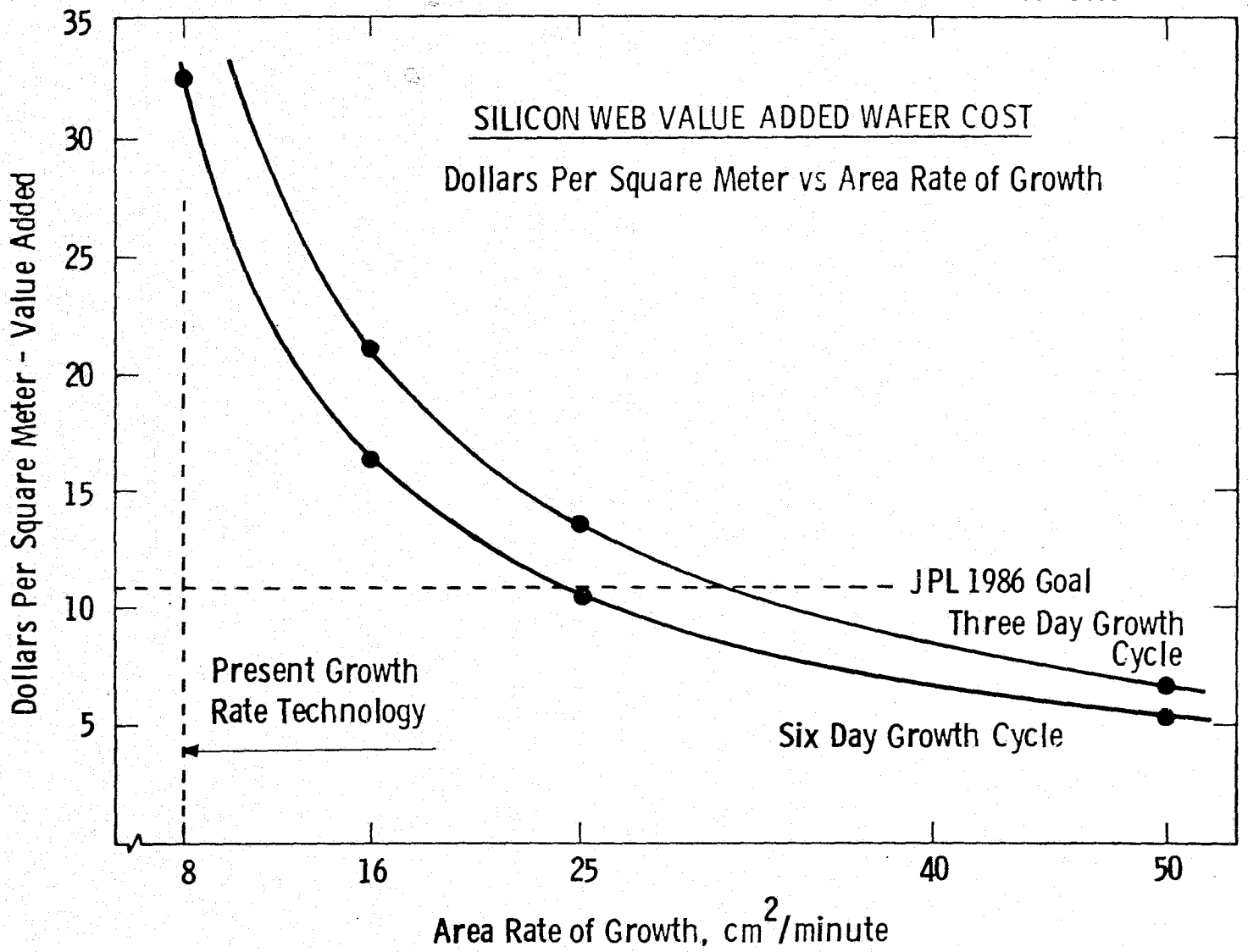

CURVE No. 6

Curve 694245-A

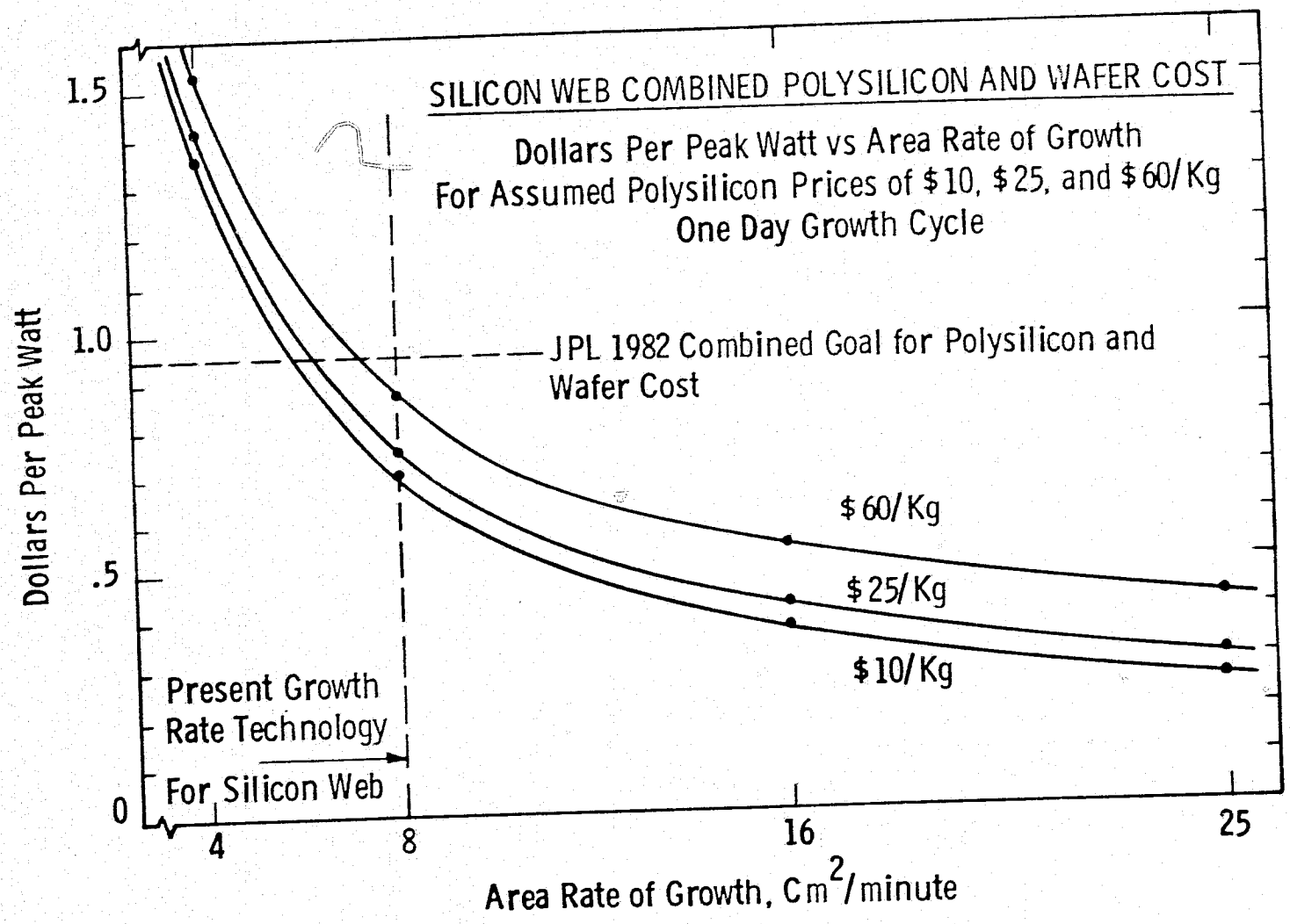

CURVE No. 1

Curve 694244-A

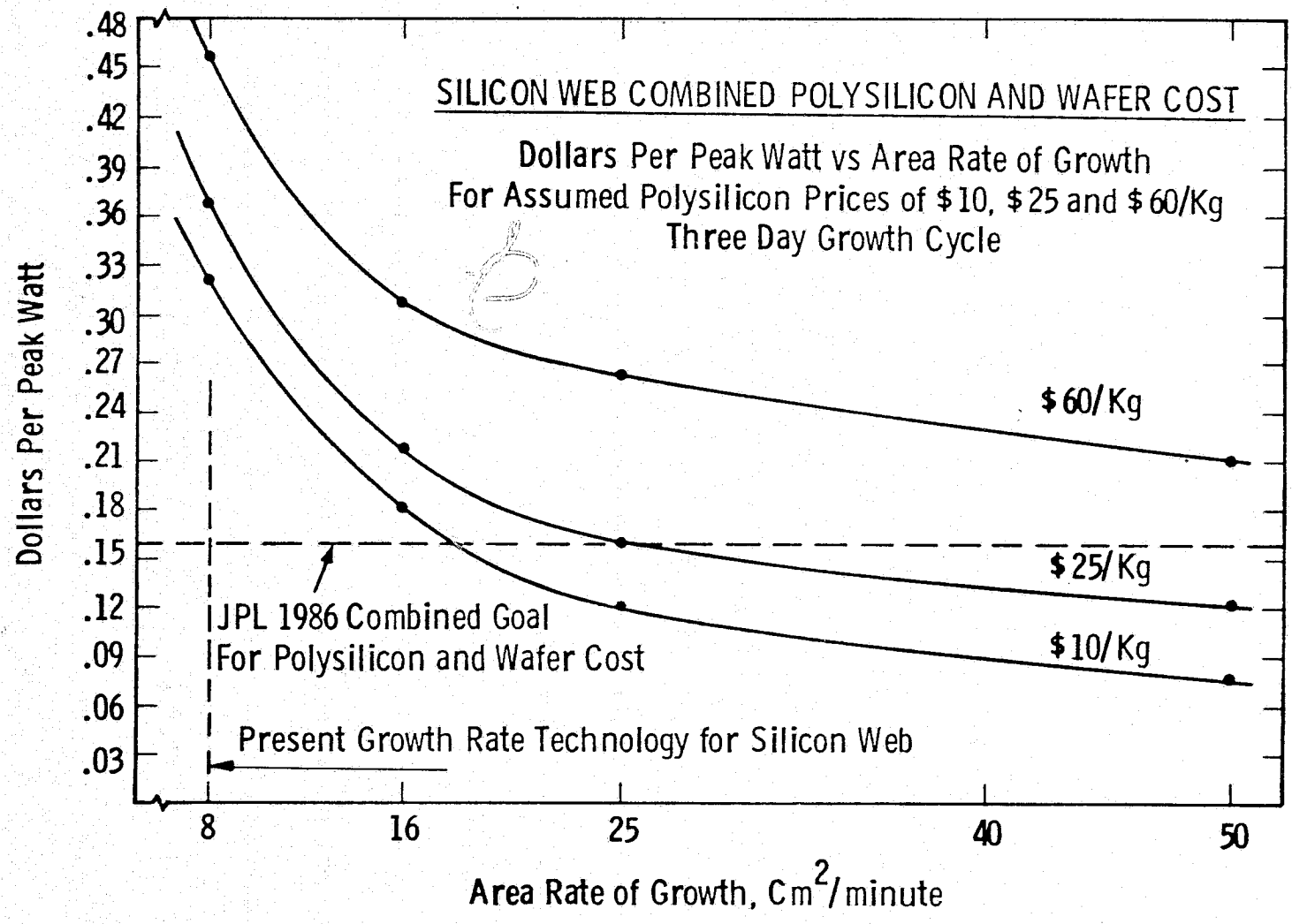

CURVE No: 8

Curve No. 8 represents the 1986 silicon web cost, indicating that the 1986 goal will be satisfied by an area growth rate of 25 cm^2 per minute and $25 per kilogram polysilicon. Ten dollars per kilogram polysilicon will satisfy the 1986 goal at an area growth rate of about 18 cm^2/minute which will require about a factor of two improvement over the present growth rate technology for silicon web.

Other Cost Considerations

This cost analysis does not include the silicon web process cost advantages which occur in later steps of solar array fabrication. As an example, solar cell efficiency determines the size and number of finished modules which must be fabricated to produce a given power rating. Encapsulation and array structure costs are likewise directly affected by cell efficiency. Thus the high cell efficiency from silicon web brings an added cost advantage. Another cost advantage results from the thinness and consequent reduced weight of silicon web.

Summary

This economic analysis shows that the silicon web process can satisfy the JPL 1982 wafer cost goal with polysilicon at 1978 prices and that further cost reduction will occur as polysilicon prices are reduced.

The analysis also shows that a factor of two improvement in the silicon web process can satisfy the 1986 wafer price goal if it is assumed that the 1986 polysilicon price goal of $10/kg is reached. In the event that a less favorable 1986 polysilicon price of $25/kg is reached, then a silicon web factor of three improvement will be required in order to reach the 1986 wafer price goal.

3. PLANS FOR THE NEXT PERIOD

In the upcoming quarter, development will be continued on the design of lids for the growth of wide, unstrained dendritic web. Emphasis will be placed on "hybrid" designs which not only yield low stress crystals but which also generate acceptable thermal conditions in the melt itself. In addition, the new dendritic growth facility will be placed into operation and growth from an elongated crucible/susceptor configuration will be investigated.

4. NEW TECHNOLOGY

No new technology occurred during this reporting period.

5. REFERENCES

1. C. S. Duncan et. al., Silicon Web Process Development: Second Quarterly Report, Contract 954654.

2. R. W. Aster & R. G. Chamberlain, LSSA Interim Price Estimation Guidelines: A Precursor and an adjunct to SAMIS III. Jet Propulsion Laboratory 5101-33, September 10, 1977.

6. APPENDIX

6.1 Growth run Detail Summary for This Reporting Period.

6.2 Susceptor Cover Slot Openings and Cross Section.

6.1

GROWTH RUN DETAIL SUMMARY

Run No.	Web No.	ΔT °C	Pull Rate cm/min	Length cm	Width mm	Thickness μm	Purpose and Comments
R-174	Melt touched lid during melt down. Aborted run.						
R-175	1	5.7	2.2	19	11.3/12.0	213	To test effect of thinner lid, 5.3 mm thick
	2	5.2	2.2	24	10.0/10.9	155	straight slot, 6.67 cm long x 7.4 mm wide
	3	6.0	2.2	28	9.0/9.9	145	new susceptor, no bottom ports
	4	5.8	1.9	58	14.7/15.4	198	101.1 gm Si, 2 x 10^{17} DOPSIL pellet
	5	4.7	1.9	29	9.6/10.0	128	excessive pullout
R-176	1	5.3	2.1	90	10.1/14.6	203	1.27 cm dia. dogbone holes added to R-175
	2	4.9	2.1	156	11.2/19.5	155	lid. 115.8 gms Si, 2 x 10^{17} DOPSIL pellet
	3	4.7	2.1	93	11.9/15.9	129	improved melt stability
R-177	1	5.4	2.2	25	10.1/11.1	178	Top shield modified on R-176 lid configur-
	2	3.3	2.1	51	10.5/13.5	178	ation. 121.3 gms Si, 2 x 10^{17} DOPSIL
	3	5.9	-	67	12.3/15.9	169	pellet. Jumpy melt
	4	5.5	1.8/1.94	32	14.1/16.2	183/152	
R-178	1	5.0	2.1	30	10.0/11.4	130	2nd top shield added to R-177 configuration
	2	4.8	1.9	107	9.8/15.8	147	110.8 gm Si, 2 x 10^{17} DOPSIL pellet
	3	3.9	1.8	73	12.3/15.5	140	oxide buildup in slot ends
	4	4.8	Thickness vs. velocity run - ice formed during growth				
R-179	Could not melt silicon, capacitors retuned.						

GROWTH RUN DETAIL SUMMARY (cont.)

Run No.	Web No.	ΔT °C	Pull Rate cm/min	Length cm	Width mm	Thickness μm	Purpose and Comments
R-180	1	5.0	2.2	103	12.8/19.0	106	Test lid configuration of R-172 without bottom ports. 121.9 gms Si, 2×10^{17} DOPSIL pellet
	2	4.5	1.9	138	12.0/19.2	111	
	3	4.5	1.8	39	12.6/14.7	138	
	4	4.6	1.8	152	13.3/19.9	107	
	5	4.4	1.7	52	13.0/14.4	117	
R-181	1	3.8	2.2	43	11.0/15.5	249	Test 10.2 cm dia. crucible, no ports in susceptor. Slot 7.62 cm long, 7.9 mm wide, with 1.59 cm dia. dogbone holes, lid 7.9 mm thick. 141.2 gm Si, 3×10^{17} DOPSIL pellet. Melt did not wet sides of crucible for 2/3 of circumference.
	2	5.2	2.5/2.9	63	14.4/19.5	225/125	
	3	3.3	2.6	15	15.2/16.4	158	
	4	4.1	2.4	29	13.1/15.8	200	

GROWTH RUN DETAIL SUMMARY (Cont.)

Run No.	Web No.	ΔT °C	Pull Rate cm/min	Length cm	Width mm	Thickness μm	Comments
R-182	Not Productive						Same configuration as R-181 (100 mm crucible) 158.9 gm Si, 3 x 10^{17} DOPSIL Si did not fill crucible to edge Melt very unstable.
R-183	1	-	2.2	22	10.5/12.0	275	Same configuration as R-181, except Top shield clearance increased 160.4 gm Si, 3 x 10^{17} DOPSIL crucible not filled to edge. Melt very unstable.
R-184	1	4.4	1.9	109	10.1/18.8	143	Lid configuration of R-172 114.2 gm Si, 2 x 10^{17} DOPSIL Return to 75 mm dia. crucible until deeper 100 mm can be obtained. Ports in bottom of susceptor.
	2	3.7	1.9	155	11.7/21.4	150	
R-185	1	4.4	2.1	116	14.0/21.5	145	Same configuration as R-184 118.5 gms Si, 2 x 10^{17} DOPSIL
	2	3.7	1.9/4.0	55	13.2/16.8	158/45	
	3	3.3	1.9	48	10.1/13.4	125	
R-186	1	2.6	2.1	184	8.5/18.5	128	Same configuration as R-184 New bottom shields installed. 122.8 gm Si, 2 x 10^{17} DOPSIL
	2	3.2	1.9	126	11.8/18.6	163	
	3	4.0	1.9	152	11.0/20.0	112	
	4	4.1	-	107	11.6/17.2		
	a	-	1.9	-	-	99	
	b	-	2.2	-	-	78	
	c	-	2.5	-	-	65	
	5	3.6	-	112	8.7/13.1		
	a	-	1.9	-	-	84	
	b	-	2.2	-	-	71	
	c	-	2.5	-	-	58	

GROWTH RUN DETAIL SUMMARY (Cont.)

Run No.	Web No.	ΔT °C	Pull Rate cm/min	Length cm	Width mm	Thickness μm	Comments
R-187	1	3.7	2.2	15	9.0/9.6	160	To test effect of wider slot
	2	4.4	2.1	15	10.7/11.0	163	6.35 cm long slot, 8 mm wide, 1.27 cm dogbone holes, 4.2 mm thick lid. 126.8 gm Si, 2 x 10^{17} DOPSIL
R-188	1	1.9	1.7	91	11.0/18.4	200	Repeat R-186
	2	2.4	1.7	140	10.8/18.3	140	118.1 gm Si, 2 x 10^{17} DOPSIL
	3	3.3	1.5	77	11.3/15.0	150	
	4	3.2	1.5	180	11.1/16.6	143	
R-189	1	3.8	1.9	51	12.0/14.2	163	Repeat R-187 Lid configuration,
	2	3.6	1.9	21	14.0/14.8	150	except use two top shields.
	3	3.7	–	180	11.3/16.7	–	125.6 gm Si, 2 x 10^{17} DOPSIL
	a	–	1.8	–	–	197	
	b	–	2.1	–	–	106	
	c	–	2.6	–	–	61	
	d	–	3.0	–	–	55	
	e	–	3.3	–	–	51	
	f	–	4.0	–	–	43	
	g	–	4.7	–	–	32	
R-190	Not Productive						Test effect of full bevel on bottom of slot in 8 mm thick lid.
R-191	1	3.8	2.1	119	11.7/19.7	180	Test thin lid with two top shields
	2	4.4	2.1	226	9.5/20.5	155	1.27 cm dia. dogbone holes on 4.45 cm
	3	3.3	1.8	148	9.2/17.5	145	centers, 6.3 mm wide slot, 4 mm thick
	a	–	1.8	–	–	114	
	b	–	2.1	–	–	88	
	c	–	2.6	–	–	56	
	d	–	3.3	–	–	42	

GROWTH RUN DETAIL SUMMARY (Cont.)

Run No.	Web. No.	ΔT °C	Pull Rate cm/min	Length cm	Width mm	Thickness μm	Purpose and Comments
R-192	1	3.8	2.1	92	11.0/14.4	188	Repeat configuration of R-191 (slot 1C)
	2	4.1	2.1	90	12.7/17.7	163	125.9 gms Si, 2 x 10^{17} DOPSIL
	3	3.9	2.1	119	8.9/15.3	110	
	4	4.1	1.9	112	13.4/18.8	120	
R-193	1	3.8	1.9	83	9.7/15.1	233	Repeat lid configuration of R-186 (7.9 mm
	2	3.9	2.2	86	12.6/16.7	143	wide slot, 22d) Ports in bottom of
	3	4.3	2.2	166	12.8/20.8	125	susceptor tapered to 16 mm dia. Slightly
	4	4.8	2.2	154	13.6/22.5	128	deeper melt 129.5 gms Si, 2 x 10^{17} DOPSIL
R-194	1	4.0	2.1	118	13.2/20.4	150	Repeat lid of R-193. Change top shield to
	2	4.6	1.9	145	12.0/21.1	153	dogbone configuration instead of straight
	3	3.2	1.9	91	11.7/12.9	110	slot. 127.0 gms. Si, 2 x 10^{17} DOPSIL
R-195	1	-	1.9	43	10.9/12.6	125	100 mm dia. new deep crucibles Same lid configuration as R-181 267.3 gms. Si, 4 x 10^{17} DOPSIL Unstable melt, ice formation
R-196	Not Productive						100 mm dia. crucible 4.3 mm Thick lid, 127 mm dia. dogbone holes on 44.4 mm centers, 2.5 x 2.5 mm bevel 275.7 gm Si, 4 x 10^{17} DOPSIL Unstable melt
R-197	Not Productive						Repeat configuration of R-196, but less Si 225.6 gm Si, 4 x 10^{17} DOPSIL Excessive oxide depostion.

GROWTH RUN DETAIL SUMMARY (Cont.)

Run No.	Web No.	ΔT °C	Pull Rate cm/min	Length cm	Width mm	Thickness μm	Purpose and Comments
R-198	Not Productive						100 mm dia. crucible, lid configuration of R-184 207.3 gms Si, 3 x 10^{17} DOPSIL Excessive oxide deposition
R-199	1	3.6	2.2	45	14.0/16.5	193	75 mm crucible. Same lid as R-196 (Slot 1A)
	2	2.9	2.2	89	10.2/15.2	140	Two Top Shields
	3	4.6	2.2	83	10.2/13.5	137	120-9 gms Si, 2 x 10^{17} DOPSIL
	4	4.1	2.2	191	9.2/18.8	126	
	5	4.4	-	76	-	-	
	a		1.5			210	
	b		2.1			99	
	c		3.1			52	
	d		4.0			36	
	6	4.7	-	94	10.1/14.1	-	
	a		3.5			35	
	b		2.1			88	
	7	4.8	2.0	36	13.4/14.6	100	
R-200	1	4.2	2.2/3.2	35	10.6/12.8	178/76	Same configuration as R-199
	2	4.3	3.2/2.2	78	12.4/15.6	76/160	120.4 gms Si, 2 x 10^{17} DOPSIL
	3	4.6	2.2/3.2	132	11.7/18.4	76/63	
	4	5.2	3.2/2.2	51	12.9/15.6	58/125	
	5	4.9	2.1	78	12.4/15.5	122	
R-201	1	4.2	2.1	29	11.0/12.5	172	75 mm crucible
	2	5.0	2.1	33	10.6/12.1	125	3.9 mm thick lid, 67 mm long slot including
	3	3.5	1.9	33	11.0/12.7	135	12.7 mm dia. dogbone holes (SLOT 3N), 6.3 mm
	4	3.3	1.9	102	11.8/17.2	114	wide

6.1

GROWTH RUN DETAIL SUMMARY (Cont.)

Run No.	Web No.	ΔT °C	Pull Rate cm/min	Length cm	Width mm	Thickness μm	Purpose and Comments
R-202	1	4.5	2.4/2.6	108	10.9/16.8	173/124	4.3 mm thick lid, 12.7 mm dogbone holes on 44.4 mm centers, 7 mm wide slot (2C) 123.0 gms Si, 2 x 10^{17} DOPSIL
R-203	1	4.1	2.1	58	9.7/12.6	165	Same configuration as R-201
	2	3.8	2.1	77	10.3/13.5	145	
	3	3.9	1.9	73	11.5/12.5	127	
	4	3.8	1.8/2.2	38	10.6/11.6	147/86	

APPENDIX 6.2

Susceptor Cover Slot Openings and Cross Sections.

WESTINGHOUSE ELECTRIC CORPORATION

SLOT 1

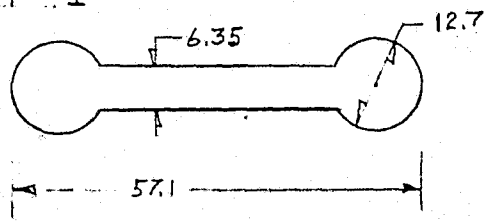

SLOT 2

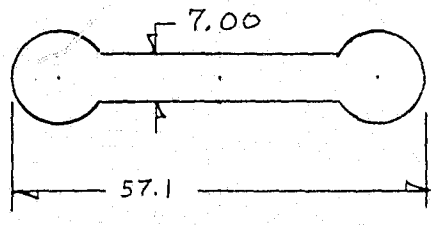

SLOT 3

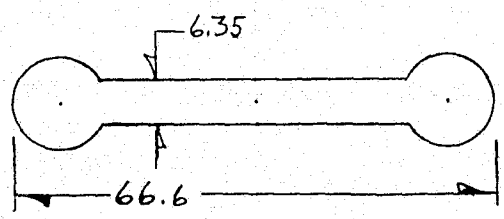

SLOT 4

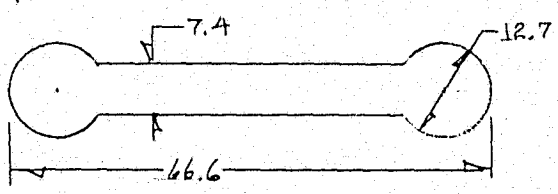

BEVEL & LID SECTIONS

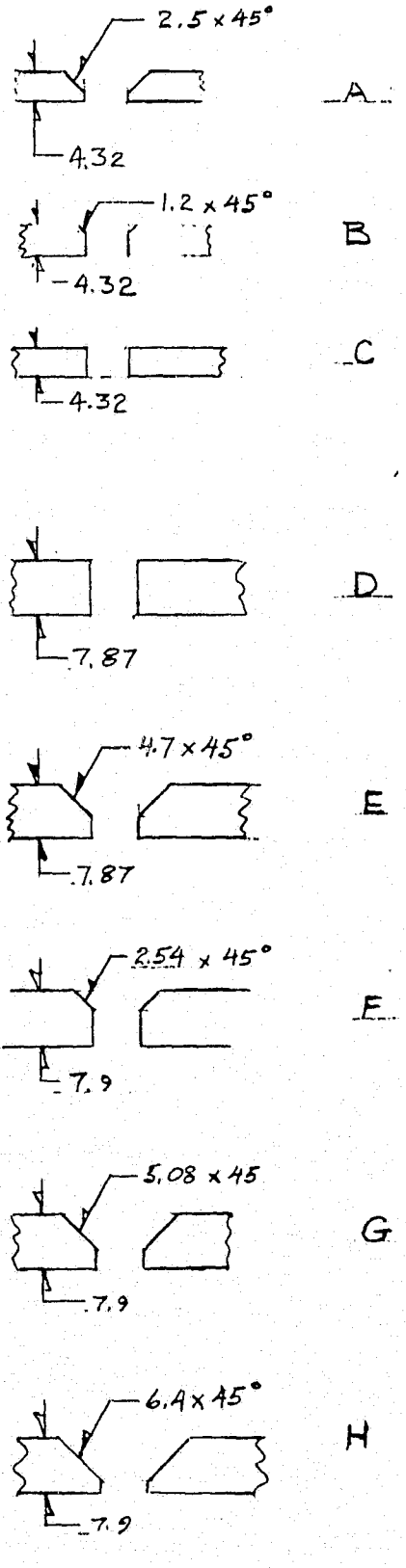

WESTINGHOUSE ELECTRIC CORPORATION

SECTION-J

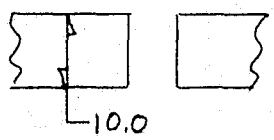

SECTION K

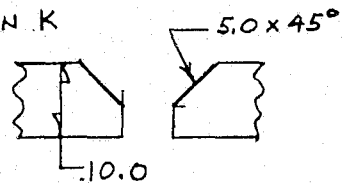

SECTION L

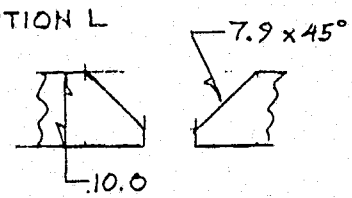

SECTION M

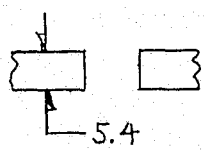

SECTION N

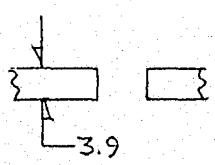

SECTION P

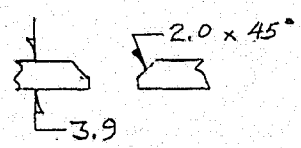

SLOT 5

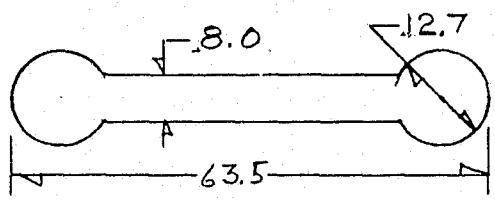

SLOT 6

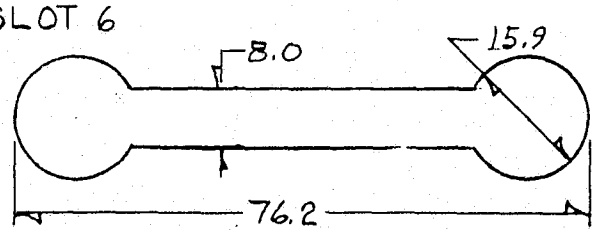

SLOT 10

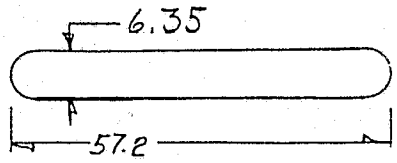

SLOT 11

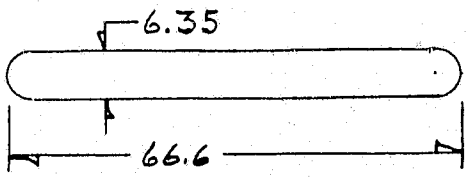

SLOT 12

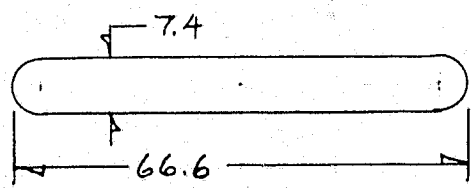

WESTINGHOUSE ELECTRIC CORPORATION

SLOT 20

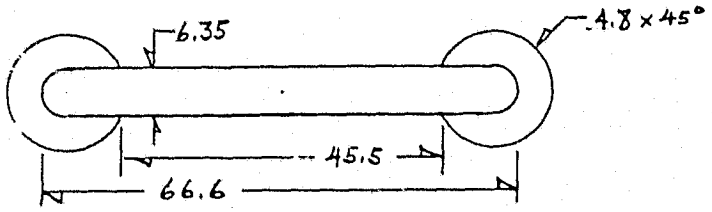

SLOT 21

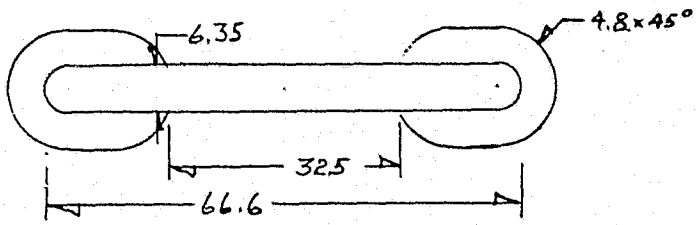

SLOT 22

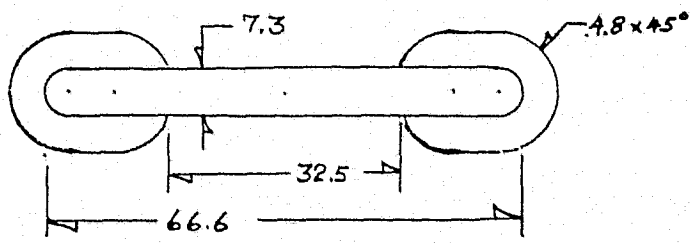

WESTINGHOUSE ELECTRIC CORPORATION

COMBINATION SLOTS. "DOGBONE" STYLE

E.G. 31JK25

SLOT 30XY-L

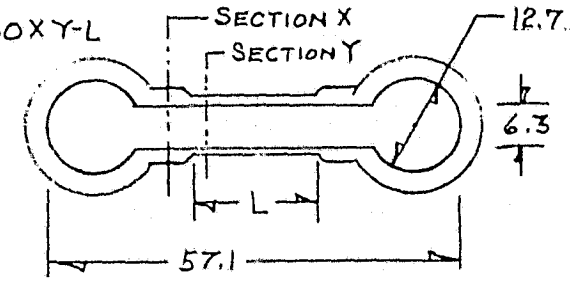

SLOT 31XY-L